IEEE TRANSACTIONS ON INDUSTRIAL ELECTRONICS, VOL. 66, NO. 3, MARCH 2019

Optimal Economic Schedule for a Network of Microgrids With Hybrid Energy Storage System Using Distributed Model Predictive Control

Felix Garcia-Torres, Carlos Bordons, *Senior Member, IEEE*, and Miguel A. Ridao, *Member, IEEE*

***Abstract*—In this paper, an optimal procedure for the economic schedule of a network of interconnected microgrids with hybrid energy storage system is carried out through a control algorithm based on distributed model predictive control (DMPC). The algorithm is specifically designed according to the criterion of improving the cost function of each microgrid acting as a single system through the network mode operation. The algorithm allows maximum economical benefit of the microgrids, minimizing the degradation causes of each storage system, and fulfilling the different system constraints. In order to capture both continuous/discrete dynamics and switching between different operating conditions, the plant is modeled with the framework of mixed logic dynamic. The DMPC problem is solved with the use of mixed integer linear programming using a piecewise formulation, in order to linearize a mixed integer quadratic programming problem.**

***Index Terms*—Distributed control, energy management, network operating systems.**

NOMENCLATURE

C	Capacity (Wh)
CC	Capital Cost (€)
Cost	Hourly economic Cost (€ /h)
Cycles	Number of life cycles
h_i	Hour i
Hours	Number of life hours
LOH	Level of Hydrogen (Nm^3)
SOC	State of Charge (p.u)
P	Electric power (W)
T_s	Sample Period
z	Electric power formulated as MLD variable (W)
δ	ON/OFF state
ε	Minimum tolerance given to the controller
η	Efficiency (p.u)
χ	Logical degradation state
ϑ	MLD power variation in degradation state (W)
(x)	Microgrid x
σ	Logical variable start up/shut down state
$(\mathcal{N})$	Network of microgrids

Subscripts:

bat	Battery
ch	Charge
degr	Degradation
dis	Discharge
elz	Electrolyzer
exch	Exchange
fc	Fuel Cell
global	Global
loss	Network losses
grid	Main grid
H_2	Hydrogen
load	Load
local	Local
neg	Negative
pos	Positive
pur	Purchase of energy
pv	Photovoltaic system
rem	Remaining power
sale	Sale of energy
uc	Ultracapacitor
wt	Wind turbine
μ grid	Microgrid

Superscripts:

$(A)->(B)$	Interaction between microgrids (A) and (B)
DM	Day-Ahead Market
on	ON state
off	OFF state
RM	Regulation Market
sch	Schedule

Manuscript received June 22, 2017; revised November 8, 2017 and February 9, 2018; accepted April 2, 2018. Date of publication May 3, 2018; date of current version October 31, 2018. This work was supported in part by the Ministry of Economy, Industry and Competitiveness of Spain under Grant DPI2016-78338-R (Project CONFIGURA), and in part by the European Commission, under the Interreg V-A Spain-Portugal Programme (POCTEP) under Grant 0076-AGERAR-6-E (Project AGERAR). *(Corresponding author: Felix Garcia-Torres.)*

F. Garcia-Torres is with the Application Unit, Centro Nacional del Hidrogeno, 13500 Puertollano, Ciudad Real, Spain (e-mail: felix.garcia@cnh2.es).

C. Bordons and M.A. Ridao are with the Systems Engineering and Automatic Control Department, Escuela de Tecnica Superior de Ingenieria, Universidad de Sevilla, 41092 Seville, Spain (e-mail: bordons@us.es; miguelridao@us.es).

Color versions of one or more of the figures in this paper are available online at http://ieeexplore.ieee.org.

Digital Object Identifier 10.1109/TIE.2018.2826476

I. Introduction

THE introduction of microgrids and energy storage system (ESS) will bring a new paradigm in the way of managing the electrical market. The interconnection of different microgrids in a network introduces flexibility to the system for both market and technical operation. The network configuration can find more advantageous situations for the different microgrid agents through the figure of an aggregator of microgrids.

The main focus of this paper is to design a procedure for the economical schedule of several interconnected microgrids, where the microgrids aggregator respects the fact that each microgrid will only act in the networked mode when the corresponding microgrid agent acquires a similar or better economic benefit than acting as a single microgrid. The method is developed with the aim to be applied to microgrids with complex cost functions, formulated as mixed integer quadratic programming (MIQP) and mixed nonlinear programing (MINLP), through a proposed method to linearize the quadratic or nonlinear terms via a piecewise approach method. With the piecewise approach, only linear constraints are obtained; with the proposed method, the controller is able to manage local cost functions (related to each microgrid as a single system), in parallel with a global cost function (related to the peer-to-peer operation of two interconnected microgrids). Later on, a procedure to extend the idea to networks of several microgrids (four in the exposed case) is also developed.

The cooperative control between microgrids has been studied in several papers and recent studies, showing its benefits toward the smart grid [1]. Nunna and Doolla [2] develop a two-level architecture for the distributed-energy-resource management for multiple microgrids using multiagent systems applying the proposed method to interconnected microgrids participating in the market with batteries as ESS. The microgrid agents in case of mismatch of demand and supply, take appropriate decision to participate in the market either as a generator agent or as a load agent. A distributed convex optimization framework is developed for energy trading between islanded microgrids in [3]. Gregoratti and Matamoros assume that all microgrids agree to cooperate with one another in order to minimize the total cost of the system. Colson and Nehrir [4] propose a decentralized control architecture for microgrids for ongoing investigations in real-time and agent-based decision-making, demonstrating the viability and capability of decentralized agent-based control for microgrids. In the negotiation process of the cited paper, an agent with lower performance may request that other agent(s) sacrifice better performance to assist in raising its own one. Fathi and Bevrani in [5] propose a negotiation process based on a defined dynamic purchase price per unit of power at each microgrid. Considering their demands and supplies, the microgrids progressively update and broadcast their prices throughout the grid. Every microgrid adaptively regulates its transactions with the rest of the grid by taking into account its realized demand as well as already announced prices from the other microgrids. In the method presented by Wu and Guan [6], each microgrid agent must coordinate in order to achieve the common goal of distribution system management under uncertainty. The control model represents a problem in which a team of decentralized decision makers, each with its own local observations of distribution system status, must cooperate together. Hug *et al.* in [7] present a method based on marginal cost functions for the negotiation process. The problem of multimicrogrids management is also treated in [8] without integrating the improvement of the status on local agents, when they are integrated in the global system.

Model predictive control (MPC) properties have drawn the attention in the research of microgrids because of its capability to handle the future behaviour of the system, demand and renewable energy generation forecasts, and systems constraints. MPC properties can be improved using a distributed formulation of the problem [9]–[11]. The dissertation carried out by Negenborn [10] discusses how control agents have to make decisions, given different constraints on the type of systems they control, the actuators they can access, the information they can sense, and the communication and cooperation they can perform. Parisio *et al.* [11] present an MPC-based distributed algorithm, aiming at coordinating an arbitrary number of microgrids, which can provide flexibility services through an aggregator. The global problem formulation introduces an additional flexibility term which represents the local remaining power capacity not utilized in the single-mode step. Muros *et al.* [12] apply a coalitional DMPC based on Shapley value. The proposed algorithm guarantees that the cost assigned to a given link is greater or lower than a certain threshold, or assures that a certain link will assume more (or less) cost than the other one. Del Real *et al.* applied DMPC to the large-scale power networks in [13] with the method of Lagrange multipliers. This optimization framework distributes overall network control effort among the local agents. Ouammi *et al.* [14] present an MPC-based procedure, formulating a global centralized control of a network of microgrids, where the objective is to maximize the overall benefits at the network level. A distributed supervisory MPC system for optimal management and operation of distributed wind and solar energy generation systems integrated into the electrical grid is carried out by Qi *et al.* in [15]. Sandgani *et al.* in [16] propose a multiobjective optimization problem which is formulated to obtain the optimal storage charge/discharge activities using a forecast of the microgrids net electricity demands within a rolling horizon control framework, without controlling the local and the global cost function.

An optimal schedule for the day-ahead, intraday and regulation service markets is applied to renewable energy microgrids with hybrid ESS using MPC techniques in [17]. Following this schedule, an optimal load sharing in the microgrid is proposed in [18].

The aforementioned studies do not consider a formulation where the cooperation between agents of microgrids provide a better status, not only for the global system (network) but also for the involved local systems (microgrids). A procedure to control both the global and local cost function is necessary to be developed. Therefore, local and global cost functions must be evaluated and the improvement in the cost function associated to networked operation must be included as a constraint.

In order to show a practical application of the method, the formulation proposed for the day-ahead and regulation service

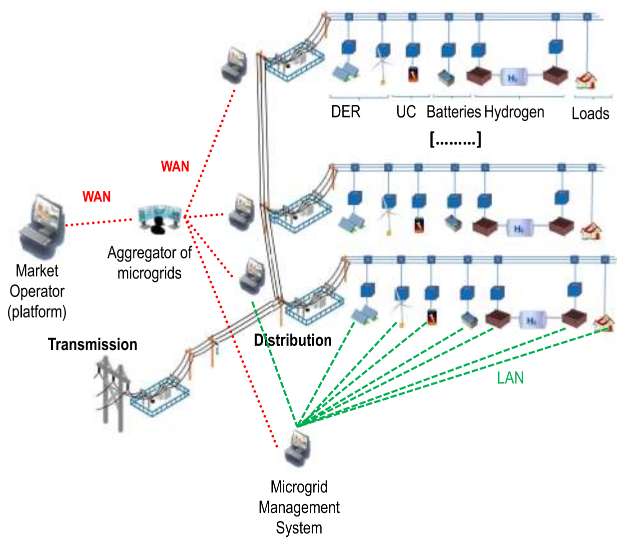

Fig. 1. Network of microgrids and communications system architecture object of this study.

TABLE I
COMPONENTS OF THE MICROGRIDS

Microgrid	(1)	(2)	(3)	(4)
PV Pannels	3 kWp	1 kWp	2 kWp	2 kWp
Wind Turbine	1 kW	3 kW	3 kW	2 kW
Electrolyzer	900 W	900 W	1000 W	2 kW
H2-Tank	7 Nm^3	7 Nm^3	7 Nm^3	14 Nm^3
Fuel Cell	600W	600 W	1000 W	2 kW
Batteries	2.7 kW 11 kWh	2.7 kW 11 kWh	6 kW 24 kWh	2.7 kW 11 kWh
Ultracapacitor	6kW 584Wh	6kW 584Wh	6kW 584Wh	6kW 584Wh
Grid Connection	2.5 kW -6 kW	2.5 kW -6 kW	6 kW -6 kW	2.5 kW -6 kW

market by Garcia-Torres and Bordons in [17] is improved using the network operation of four coupled microgrids. The design criterion is that the microgrid should only exchange energy with the network if its local cost function is improved. This concept guarantees a better status of the microgrid components and operation, acting as part of the network than acting as a single microgrid. In the case of the Regulation Market, the algorithm searches equitable gains for the microgrids of the network. These issues have not been studied in the existing literature, being the major contribution of this paper. The network of microgrids object of this paper is shown in Fig. 1 and Table I. As can been seen in Fig. 1, all the microgrids and the aggregator of microgrids are communicated via WAN. The aggregator of microgrids centralizes the communication with the market operator.

This paper is organized as follows. Section II exposes the controller design. Section III presents the results of the energy schedule carried out by the DMPC controllers. Finally, Section IV outlines the conclusions.

II. Day-Ahead DMPC Controller

This section describes the methodology, that consists of finding the best exchange of energy between the microgrids. The proposed algorithm is composed of three main parts: 1) the optimization of the microgrids as single systems; 2) the improvement of the economic benefit of each microgrid using a peer-to-peer procedure; and 3) evaluation of all the possible combinations of pair of microgrids in the network, in order to find the best exchange of energy inside the network of microgrids.

A. Single Microgrid Optimization

The day-ahead market optimization local problem for the microgrid x can be defined as follows (see [17]):

$$J_{\text{local}}^{\text{DM},(x)} = J_{\text{grid,local}}^{\text{DM},(x)} + J_{\text{bat,local}}^{\text{DM},(x)} + J_{H_2,\text{local}}^{\text{DM},(x)}. \tag{1}$$

The cost function of energy exchange with the main grid in the day-ahead market is defined as follows [17]:

$$J_{\text{grid,local}}^{\text{DM},(x)}(h_i) = \sum_{h_i=1}^{24} \left(-\Gamma_{\text{sale}}^{\text{DM}}(h_i) \cdot P_{\text{sale}}(h_i) + \Gamma_{\text{pur}}^{\text{DM}}(h_i) \cdot P_{\text{pur}}(h_i)\right) \cdot T_s \tag{2}$$

where $\Gamma_{\text{sale}}^{\text{DM}}(h_i)$ and $\Gamma_{\text{pur}}^{\text{DM}}(h_i)$ are the predicted hourly energy prices. $P_{\text{pur}}(h_i)$ and $P_{\text{sale}}(h_i)$ are the exchange of the power to be purchased or sold to the grid.

The battery operation in the microgrid should minimize the number of cycles of charge and discharge [first terminus of (3)] but should also avoid high current ratio in the charging and discharging process [second terminus of (3)] [17]:

$$J_{\text{bat,local}}^{\text{DM},(x)}(h_i) = \sum_{h_i=1}^{24} \left(\frac{\text{CC}_{\text{bat}}}{2 \cdot \text{Cycles}_{\text{bat}} \cdot C_{\text{bat}}} P_{\text{bat,ch}}(h_i) \cdot T_s \cdot \eta_{\text{bat,ch}} + \frac{\text{CC}_{\text{bat}}}{2 \cdot \text{Cycles}_{\text{bat}} \cdot C_{\text{bat}}} \frac{P_{\text{bat,dis}}(h_i) \cdot T_s}{\eta_{\text{dis,bat}}} + \text{Cost}_{\text{degr}} \cdot P_{\text{bat}}^2(h_i) \right) \tag{3}$$

where CC_{bat} refers to the capital cost of the batteries, $\text{Cycles}_{\text{bat}}$ means the number of life cycles given by the manufacturer, and $\eta_{\text{dis,bat}}$ and $\eta_{\text{ch,bat}}$ are the efficiencies for the charging and discharging process of the batteries. The terms $P_{\text{ch,bat}}$ and $P_{\text{dis,bat}}$ are the power of charging or discharging of the batteries. The term $P_{\text{bat}} = P_{\text{ch,bat}} - P_{\text{dis,bat}}$ is the net power that the batteries exchange with the microgrid. Finally, $\text{Cost}_{\text{degr}}$ is a factor to penalize the degradation process of the batteries due to high stress in the charging and discharging process. In the case of the hydrogen ESS, the number of working hours for the electrolyzer and fuel cell $(\delta_{\text{elz}}, \delta_{\text{fc}})$ must be minimized, as well as the start-up and shut-down cycles $(\sigma_{\text{elz}}, \sigma_{\text{fc}})$. Once the electrolyzer or the fuel cell are started, the power fluctuations $(\vartheta_{\text{elz}}, \vartheta_{\text{fc}})$ must also be minimized.

$$J_{H_2,\text{local}}^{\text{DM},(x)}(h_i) = \sum_{\alpha=\text{elz,fc}} \left(\text{Cost}_{\text{degr},\alpha} \cdot \vartheta_\alpha^2(h_i) + \left(\frac{\text{CC}_\alpha}{\text{Hours}_\alpha} + \text{Cost}_{\text{o\& m},\alpha} \right) \delta_\alpha(h_i) + \text{Cost}_{\text{startup},\alpha} \cdot \sigma_\alpha^{\text{on}}(h_i) + \text{Cost}_{\text{shutdown,elz}} \cdot \sigma_\alpha^{\text{off}}(h_i) \right) \tag{4}$$

where CC_α are the capital costs of the electrolyzer and fuel cell, Hours_α are the number of life hours given by the manufacturers, and $\text{Cost}_{\text{o\& m},\alpha}$ are the costs of operation and maintenance of these devices. $\text{Cost}_{\text{startup},\alpha}$, $\text{Cost}_{\text{shutdown},\alpha}$, and $\text{Cost}_{\text{degr},\alpha}$ are the costs associated to the degradation processes of start up, shut down, and power fluctuations.

The solver finds an optimal solution for each microgrid as a single system giving an optimal set of the control variables: $\mathbf{U}^{\text{opt}}_{\text{local}} = [P^{\text{opt}}_{\text{grid,local}}(h_i)\ P^{\text{opt}}_{\text{bat,local}}(h_i)\ \delta^{\text{opt}}_{\text{elz,local}}(h_i)\ \delta^{\text{opt}}_{\text{fc,local}}(h_i)\ z^{\text{opt}}_{\text{elz,local}}(h_i)\ z^{\text{opt}}_{\text{fc,local}}(h_i)]$.

B. Peer-to-Peer Optimization

The cost function introduced in (1) can be expanded to a global cost function for two coupled microgrids as follows:

$$J^{\text{DM}}_{\text{global}} = \sum_{x=A,B} J^{\text{DM},(x)}_{\text{local}}. \tag{5}$$

The following constraints must be added in order to introduce the link restrictions between the different microgrids:

$$P^{(A)\to(B)}(h_i) + P^{(B)\to(A)}(h_i) = 0 \tag{6}$$

where $P^{(x)\to(y)}(h_i)$ is the power flow between microgrid (x) and microgrid (y). The interchange of energy between two microgrids is subject to transport losses which can be modeled as follows:

$$P^{(A)\to(B)}(h_i) = P^{(A)\to(B)}_{\text{exch}}(h_i) + P^{(A)\to(B)}_{\text{loss}}(h_i). \tag{7}$$

In case the energy is flowing from microgrid (A) towards microgrid (B) $P^{(A)->(B)} > 0$, the absolute value of the energy received by (B) $P^{(B)->(A)}_{\text{exch}} > 0$ is equal to the energy which is leaving from microgrid (A) $P^{(A)->(B)} > 0$, minus the losses of the network transport $P^{(B)->(A)}_{\text{loss}} > 0$. In order to follow this nomenclature, the energy losses are zero in case the exchange of energy is flowing out of one microgrid. This can be expressed with the following expressions:

$$\delta^{(A)->(B)}_{\text{pos}}(h_i) = \begin{cases} 1 & P^{(A)->(B)}(h_i) > 0 \\ 0 & P^{(A)->(B)}(h_i) \le 0 \end{cases} \tag{8}$$

$$\delta^{(A)->(B)}_{\text{neg}}(h_i) = \begin{cases} 1 & P^{(A)->(B)}(h_i) < 0 \\ 0 & P^{(A)->(B)}(h_i) \ge 0 \end{cases} \tag{9}$$

$$z^{(A)->(B)}_{\text{pos}}(h_i) = \delta^{(A)->(B)}_{\text{pos}}(h_i) \cdot P^{(A)->(B)}(h_i) \tag{10}$$

$$z^{(A)->(B)}_{\text{neg}}(h_i) = \delta^{(A)->(B)}_{\text{neg}}(h_i) \cdot (P^{(A)->(B)}(h_i)) \tag{11}$$

$$P^{(A)->(B)}_{\text{loss}}(h_i) = \eta^{(A)->(B)}_{\text{loss}} \cdot z^{(A)->(B)}_{\text{neg}}(h_i). \tag{12}$$

When the two microgrids are working as a network, the physical constraints of the optimization problem must be reformulated from the expression introduced in the constraints (31)–(35) of [17] as follows:

$$\sum_{x=A,B}\sum_{y=\text{pv,wt}} P^{(x)}_y(h_i) - P^{(A)->(B)}_{\text{loss}} - P^{(B)->(A)}_{\text{loss}}$$
$$= \sum_{x=A,B}\left(\sum_{y=\text{grid,bat,load}} P^{(x)}_y(h_i) + z^{(x)}_{\text{elz}}(h_i) - z^{(x)}_{\text{fc}}(h_i)\right) \tag{13}$$

$$P^{\min,(x)}_i \le P^{(x)}_i(h_i) \le P^{\max,(x)}_i|^{x=A,B}_{i=\text{grid,elz,fc,bat}} \tag{14}$$

$$\text{SOC}^{\min,(x)}_{\text{bat}} \le \text{SOC}^{(x)}_{\text{bat}}(h_i) \le \text{SOC}^{\max,(x)}_{\text{bat}}|^{x=A,B} \tag{15}$$

$$\text{LOH}^{\min,(x)} \le \text{LOH}^{(x)}(h_i) \le \text{LOH}^{\max,(x)}|^{x=A,B} \tag{16}$$

$$0 \le \delta^{(x)}_i(h_i) \le 1|^{x=A,B}_{i=\text{elz,fc}}. \tag{17}$$

Taking this consideration, the energy balance equation for each microgrid can be reformulated from the constraint introduced in (31) of [17], as follows [formulated for microgrid (A), similar procedure for microgrid (B)]:

$$P^{(A)}_{\text{pv}}(h_i) + P^{(A)}_{\text{wt}}(h_i) - P^{(A)}_{\text{load}}(h_i) = P^{(A)}_{\text{grid}}(h_i)$$
$$+ z^{(A)}_{\text{elz}}(h_i) - z^{(A)}_{\text{fc}}(h_i) + P^{(A)}_{\text{bat}}(h_i) + P^{(A)\to(B)}(h_i). \tag{18}$$

The solution given by the global function of the P2P operation must provide a more advantageous situation with respect to working as a single microgrid. The solution of the control problem for a network of two microgrids [microgrid (A) and microgrid (B)] gives a set of optimal control variables composed by $\mathbf{U}^{\text{opt}}_{\text{global}} = [\mathbf{U}^{\text{opt},(A)}_{\text{global}}, \mathbf{U}^{\text{opt},(B)}_{\text{global}}, P_{(A)->(B)}]$. An agreement is found when the next constraints are satisfied as

$$J^{\text{DM},(A)}_{\text{local}}(\mathbf{U}^{\text{opt},(A)}_{\text{global}}) <= J^{\text{DM},(A)}_{\text{local}}(\mathbf{U}^{\text{opt},(A)}_{\text{local}}) \tag{19}$$

$$J^{\text{DM},(B)}_{\text{local}}(\mathbf{U}^{\text{opt},(B)}_{\text{global}}) <= J^{\text{DM},(B)}_{\text{local}}(\mathbf{U}^{\text{opt},(B)}_{\text{local}}). \tag{20}$$

To accomplish the constraint given by (19) and (20) the problem should be formulated as a Mixed-Integer Quadratic programming problem with Quadratic constraints. However, this kind of formulation takes higher complexity and solving time for the control problem. In the case of $\vartheta^2_{\text{elz}}(h_i)$ and $\vartheta^2_{\text{fc}}(h_i)$, these terms were utilized just to minimize the absolute value of these variables. In [17] the variables χ_i and ϑ_i are defined as follows:

$$\chi_\alpha(h_i) = \delta_\alpha(h_i) \wedge \delta_\alpha(h_{i-1})|_{\alpha=\text{elz,fc}} \tag{21}$$

$$\vartheta_\alpha(h_i) = \Delta P_\alpha(h_i) \cdot \chi_\alpha(h_i)|_{\alpha=\text{elz,fc}}. \tag{22}$$

Four new logical variables are introduced to differentiate between the negative and positive increments of power in the electrolyzer and the fuel cell:

$$\delta^-_\alpha(h_i) = 1 \iff \Delta P_\alpha(h_i) \le 0|_{\alpha=\text{elz,fc}} \tag{23}$$

$$\delta^+_\alpha(h_i) + \delta^-_\alpha(h_i) = 1|_{\alpha=\text{elz,fc}} \tag{24}$$

$$\chi^{\text{sign}}_\alpha(h_i) = 1 \iff \delta^{\text{sign}}_\alpha(h_i) \wedge \chi_\alpha(h_i)|^{\text{sign}=+,-}_{\alpha=\text{elz,fc}} \tag{25}$$

$$\vartheta^{\text{sign}}_\alpha(h_i) = \Delta P_\alpha(h_i) \cdot \chi^{\text{sign}}_\alpha(h_i)|^{\text{sign}=+,-}_{\alpha=\text{elz,fc}}. \tag{26}$$

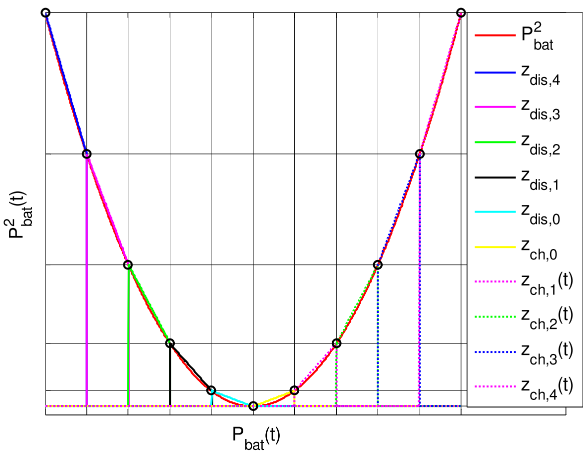

Fig. 2. Linear-piecewise representation of P^2_{bat}.

The quadratic term $P^2_{\text{bat}}(h_i)$ used in [17] was introduced to penalize high values of $P_{\text{bat}}(h_i)$, in order to minimize the degradation process due to the exposition of the batteries to high levels of charge or discharge currents. The quadratic expression of $P_{\text{bat}}(h_i)$ is linearized using a piecewise expression composed of ten parts, see (27) and (28) and Fig. 2 (Notice that the proposed linearization method can be applied with more or less parts depending of the precision or the linear approach required).

$$P_{\text{bat}}(h_i) = \sum_{n=0}^{n=4} (z_{\text{ch},n}(h_i) - z_{\text{dis},n}(h_i)) \tag{27}$$

$$z_{\alpha,n}(h_i) = P_{\alpha,n}(h_i) \cdot \delta_{\alpha,n}(h_i)|^{\alpha=\text{ch,dis}}_{n=0,..,4}. \tag{28}$$

The next constraints are imposed to the MPC-controller

$$P_{\alpha,n-1,\max} \le P_{\alpha,1}(h_i) \le P_{\alpha,n,\max}|^{n=1,\dots,4}_{\alpha=\text{ch,dis}}. \tag{29}$$

Only one part of the piecewise function can be active, so the next set of constraints is imposed to the logical variables of (27) and (28).

$$0 \le \delta_{\alpha,n}(h_i) + \delta_{\beta,m}(h_i) \le 1|^{n,m=0,1,2,3,4}_{\alpha,\beta=\text{ch,dis}}. \tag{30}$$

These constraints must be satisfied in all the cases, where $\delta_{\alpha,n}(h_i) \neq \delta_{\beta,m}(h_i)$. The quadratic expression of $P_{\text{bat}}(h_i)$ is linearized with its piecewise expression as follows:

$$P^2_{\text{bat}}(h_i) \approx \sum_{n=0}^{n=4} (A_{\text{ch},n} \cdot z_{\text{ch},n} + B_{\text{ch},n} \cdot \delta_{\text{ch},n} + A_{\text{dis},n} \cdot z_{\text{dis},n} + B_{\text{ch},n} \cdot \delta_{\text{dis},n}) \tag{31}$$

$$A_{\alpha,n} = \frac{P^2_{\alpha,n,\max} - P^2_{\alpha,n,\min}}{P_{\alpha,n,\max} - P_{\alpha,n,\min}}|^{\alpha=\text{ch,dis}}_{n=0,1,2,3,4} \tag{32}$$

$$B_{\alpha,n} = \frac{P^2_{\alpha,n,\max} - P^2_{\alpha,n,\min}}{P_{\alpha,n,\max} - P_{\alpha,n,\min}} \cdot (-P_{\alpha,n,\min}) + P^2_{\alpha,n,\min}|^{\alpha=\text{ch,dis}}_{n=0,1,2,3,4}. \tag{33}$$

The expressed cost function for the batteries and hydrogen used in [17] can be reformulated without any quadratic term.

$$J^{\text{DM},(x)}_{\text{bat,local}}(h_i) = \sum_{h_i=1}^{24} \left(\frac{\text{CC}_{\text{bat}} \cdot T_s \cdot \eta_{\text{bat,ch}}}{2 \cdot \text{Cycles}_{\text{bat}} \cdot C_{\text{bat}}} \left(\sum_{n=0}^{n=4} z_{\text{bat,ch},n}(h_i) \right) + \frac{\text{CC}_{\text{bat}}}{2 \cdot \text{Cycles}_{\text{bat}} \cdot C_{\text{bat}}} \frac{T_s}{\eta_{\text{dis,bat}}} \cdot \left(\sum_{n=0}^{n=4} z_{\text{bat,dis},n}(h_i) \right) \sum_{\alpha=\text{ch,dis}} \sum_{n=0}^{n=4} \text{Cost}_{\text{degr}} \cdot (A_{\alpha,n} \cdot z_{\alpha,n} + B_{\alpha,n} \cdot \delta_{\alpha,n}) \right) \tag{34}$$

$$J^{\text{DM},(x)}_{H_2,\text{local}}(h_i) = \sum_{\alpha=\text{elz,fc}} \left(\left(\frac{\text{CC}_{\text{elz}}}{\text{Hours}_\alpha} + \text{Cost}_{\text{o\& m},\alpha} \right) \delta_\alpha(h_i) + \text{Cost}_{\text{degr},\alpha} \cdot (\vartheta^+_\alpha(h_i) + \vartheta^-_\alpha(h_i)) + \text{Cost}_{\text{startup},\alpha} \cdot \sigma^{\text{on}}_\alpha(h_i) + \text{Cost}_{\text{shutdown},\alpha} \cdot \sigma^{\text{off}}_\alpha(h_i) \right). \tag{35}$$

Finally, in order to optimize the power transactions between the two microgrids, the power flow between them must be minimized with a small weighting factor in the global cost function. The global cost function introduced in (5) must be redefined as follows:

$$J^{\text{DM}}_{\text{global}} = \sum_{[(x,y)=A,B;(x,y)=B,A]} \left(J^{\text{DM},(x)}_{\text{local}} + w^{(x)->(y)} \cdot (z^{(x)->(y)}_{\text{pos}}(h_i) - z^{(x)->(y)}_{\text{neg}}(h_i)) \right). \tag{36}$$

C. Network Optimization

The high number of constraints to be introduced in the controller makes it unfeasible (using standard computational hardware) to solve the network optimization problem with a number of microgrids higher than just two microgrids in a centralized way.

The proposed algorithm computes the power exchange among microgrids, selecting the most promising couple of microgrids in a sequential fashion, as explained in the following.

First, all possible couples of microgrids are evaluated using the algorithm described in Section II-B. The number of couple evaluations is $(N_{\mu\text{grids}} - 1)!$ where $N_{\mu\text{grids}}$ is the number of microgrids in the network. Only couples of microgrids where the value of the global function is lower than the sum of its local cost functions are considered (feasible couples). Then, among these feasible couples, the one with the highest decrement is selected. If microgrids i and j form the selected couple, this step fixed the power exchange between microgrid i and microgrid j, $P^{(i)\to(j)}$.

In the next step, the couples evaluation is performed again eliminating the couple (i,j), that is, $(N_{\mu\text{grids}} - 1)! - 1$ combinations are considered. A new couple (k,l) is selected and $P^{(k)\to(l)}$ is fixed. So the energy balance constraint for each microgrid mentioned in (18) has to be replaced as follows:

$$\begin{aligned} &P_{\text{pv}}^{(x)}(h_i) + P_{\text{wt}}^{(x)}(h_i) - P_{\text{load}}^{(x)}(h_i) \\ &\quad - \sum_{M=1,\ldots,N_{\text{ITERS}}-1} \sum_{\alpha=1,\ldots,N_{\mu\text{ grids}}} P^{(x)\to(\alpha)}(h_i)|_{\text{ITER}-M} \\ &= P_{\text{grid}}^{(x)}(h_i) + z_{\text{elz}}^{(x)}(h_i) - z_{\text{fc}}^{(x)}(h_i) \\ &\quad + P_{\text{bat}}^{(x)}(h_i) + P_{\text{uc}}^{(x)}(h_i) + P^{(x)\to(y)}(h_i). \end{aligned} \tag{37}$$

The term $P^{(x)\to(\alpha)}(h_i)|_{\text{ITER}-M}$ refers to the exchange of energy between the microgrids of a selected couple in the previous iteration.

This algorithm continues until a new feasible couple cannot be found in a given step, or all the links have been selected.

$$P^{(x)\to(y)}(h_i) = 0 \quad \forall (x),(y) \in \mathcal{N}. \tag{38}$$

III. Regulation Service DMPC Controller

The cost function of the Regulation Service Market formulated in [17] can be reformulated for the P2P operation of two microgrids linearizing all the terms ($T_s = 10$ min and the control horizon 3 h.)

$$\begin{aligned} J_{\text{global}}^{\text{RM}}(t_k) = &\sum_{[(x,y)=A,B;(x,y)=B,A]} \Big(J_{\text{local}}^{\text{RM},(x)}(t_k) \\ &+ w^{(x)->(y)} \cdot \left(z_{\text{pos}}^{\text{RM},(x)->(y)}(t_k) + z_{\text{neg}}^{\text{RM},(x)->(y)}(t_k) \right) \Big) \end{aligned} \tag{39}$$

$$\begin{aligned} &J_{\text{grid}}^{RM,(x)}(t_k) = \\ &\sum_{j=1}^{j=18} \left(\Gamma_{\text{up}}^{\text{RM}}(t_{k+j}) \cdot \text{dev}P_{\text{grid}}(t_{k+j}) \cdot \delta_{\text{up,grid}}(t_{k+j}) \right. \\ &\quad \left. -\Gamma_{\text{down}}^{\text{RM}}(t_{k+j}) \cdot \text{dev}P_{\text{grid}}(t_{k+j}) \cdot \delta_{\text{down,grid}}(t_{k+j}) \right) \end{aligned} \tag{40}$$

$$\text{dev}P_{\text{grid}}(t_{k+j}) = P_{\text{grid}}(t_{k+j}) - P_{\text{grid}}^{\text{DM}}(t_{k+j}) \tag{41}$$

$$\begin{aligned} J_{\text{uc}}^{\text{RM},(x)}(t_k) = &\sum_{j=1}^{18} \left(w_{\text{uc}} \cdot \text{devSOC}_{\text{uc}}(t_{k+j}) \cdot \delta_{\text{up,uc}}(t_k) \right. \\ &\left. w_{\text{uc}} \cdot \text{devSOC}_{\text{uc}}(t_{k+j}) \cdot \delta_{\text{down,uc}}(t_k) \right) \end{aligned} \tag{42}$$

$$\text{devSOC}_{\text{uc}}(t_k) = \text{SOC}_{\text{uc}}(t_k) - \text{SOC}_{\text{uc}}^{\text{ref}} \tag{43}$$

where $\delta_{\text{up,grid}}(t_k)$ and $\delta_{\text{up,uc}}(t_k)$ are active, when the $\text{dev}P_{\text{grid}}(t_k)$ or $\text{devSOC}_{\text{uc}}(t_k)$ are positive; and $\delta_{\text{down,grid}}(t_k)$ and $\delta_{\text{down,uc}}(t_k)$ are active, when the $\text{dev}P_{\text{grid}}(t_k)$ or $\text{devSOC}_{\text{uc}}(t_k)$ are negative.

$$\begin{aligned} &J_{\text{bat}}^{\text{RM},(x)}(t_k) = \\ &\sum_{j=1}^{18} \left(w_{\text{bat}} \cdot \left(\text{SOC}_{\text{bat}}(t_{k+j}) - \text{SOC}_{\text{bat}}^{\text{sch}}\right) \cdot \delta_{up,\text{bat}}(t_k) \right. \\ &\left. w_{\text{bat}} \cdot \left(\text{SOC}_{\text{bat}}(t_{k+j}) - \text{SOC}_{\text{bat}}^{\text{sch}}\right) \cdot \delta_{\text{down,bat}}(t_k) \right) \\ &+ \frac{1}{6} \sum_{j=1}^{j=18} \left(\frac{\text{CC}_{\text{bat}}}{2 \cdot \text{Cycles}_{\text{bat}} \cdot C_{\text{bat}}} \left(\frac{P_{\text{bat,dis}}(t_{k+j})}{\eta_{\text{dis,bat}}} \right.\right. \\ &\left.\left. + P_{\text{bat,ch}}(t_{k+j}) \cdot \eta_{\text{bat,ch}} \right) \right) \\ &+ w_{\text{degr}} \sum_{x=\text{ch,dis}} \sum_{n=0}^{n=4} \left(A_{x,n} \cdot z_{x,n}(t_{k+j}) + B_{x,n} \cdot \delta_{x,n}(t_{k+j}) \right) \end{aligned} \tag{44}$$

$$\begin{aligned} &J_{H_2,\text{local}}^{\text{RM},(x)}(t_k) = \\ &\sum_{j=1}^{18} \left(w_{H_2} \cdot \left(\text{LOH}(t_{k+j}) - \text{LOH}_{\text{bat}}^{\text{sch}}\right) \cdot \delta_{\text{up},H_2}(t_k) \right. \\ &\quad \left. w_{H_2} \cdot \left(\text{LOH}(t_{k+j}) - \text{LOH}^{\text{sch}}\right) \cdot \delta_{\text{down},H_2}(t_k) \right) \\ &+ \sum_{\alpha=\text{elz,fc}} \left(\sum_{j=1}^{j=18} \left(\frac{1}{6} \left(\frac{\text{CC}_\alpha}{\text{Hours}_\alpha} + \text{Cost}_{\text{o\& m},\alpha} \right) \delta_\alpha(t_{k+j}) \right.\right. \\ &+ w_{\text{startup},\alpha} \cdot \sigma_\alpha^{\text{on}}(t_{k+j}) + w_{\text{shutdown},\alpha} \cdot \sigma_\alpha^{\text{off}}(t_{k+j}) \\ &\left.\left. + \text{Cost}_{\text{degr},\alpha} \cdot \left(\vartheta_\alpha^+(h_i) + \vartheta_\alpha^-(h_i)\right) \right) \right). \end{aligned} \tag{45}$$

In order to find an equitable gain between the two microgrids which form a couple, the agreement in the regulation service market is similar to the day-ahead market as follows:

$$\begin{aligned} &J_{\text{local}}^{\text{RM},(A)}(\mathbf{U}_{\text{global}}^{\text{opt},(A)}) - J_{\text{local}}^{\text{RM},(A)}(\mathbf{U}_{\text{local}}^{\text{opt},(A)}) \\ &\quad = J_{\text{local}}^{\text{RM},(B)}(\mathbf{U}_{\text{global}}^{\text{opt},(B)}) - J_{\text{local}}^{\text{RM},(B)}(\mathbf{U}_{\text{local}}^{\text{opt},(B)}). \end{aligned} \tag{46}$$

Similar procedure is carried out in the case of the day-ahead market for the network operation of the regulation market.

IV. Results and Discussion

The proposed controller has been developed using the solver TOMLAB/CPLEX. The values for the parameters of the controller are given in Table II.

A. Day-Ahead P2P Controller

In order to validate and show the results of the P2P controller, it is applied to two identical microgrids with the values of microgrid (1) (see Table I). The evolution of the prices in the day-ahead market (obtained by an artificial neural network forecast algorithm) is presented in Fig. 3. In Figs. 4–9 and Table III, a comparison between the results of the different controllers is shown. In the first instance, a comparison between the original schedule method given by an MIQP formulation for a single microgrid proposed in [17] and its comparison with the

TABLE II
VALUES OF THE CONTROLLER

Electrolyzer: $\text{Cost}_{degr,elz} = 0.0577$ €$/W$, Lifetime= 10000 hours $\varsigma = 0.23\ Nm^3/kWh$, CC= 8.22 €$/kW$, $\text{Cost}_{o\&m,elz} = 0.002$ €$/h$ $\text{Cost}_{startup,elz} = 0.123$ €, $\text{Cost}_{shutdown,elz} = 0.0062$ €
Fuel Cell: $\text{Cost}_{degr,fc} = 0.0018$ €$/W$, Lifetime= 10000 hours $\varsigma = 1.320\ kWh/Nm^3$, CC=30 €$/kW$, $\text{Cost}_{o\&m,fc} = 0.001$ €$/h$ $\text{Cost}_{startup,fc} = 0.01$ €, $\text{Cost}_{shutdown,fc} = 0.005$ €,
Batteries: $\eta_{ch} = 0.90$, $\eta_{dis} = 0.95$, CC=125 €/kWh, Life cycles=3000, $\text{Cost}_{degr,dis} = 10^{-9}$ €$/W^2h$, $\text{Cost}_{degr,ch} = 10^{-9}$ €$/W^2h$
Ultracapacitor: $\eta_{ch} = 0.99$, $\eta_{dis} = 0.98$

Data based on U.S. Department of Energy (DOE) final targets [20], [21] and [22]

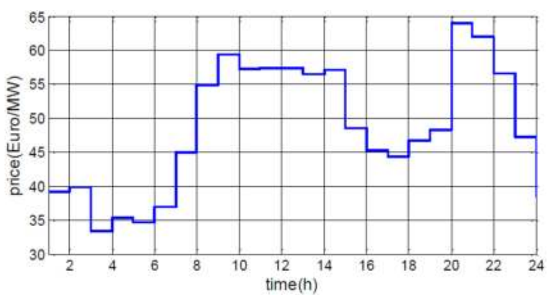

Fig. 3. Price evolution per hour.

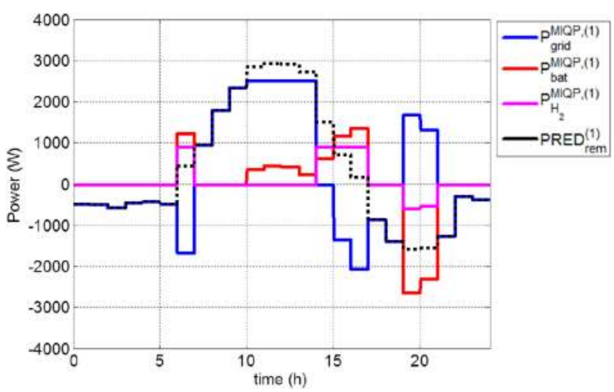

Fig. 4. Day-ahead optimization results obtained for Microgrid (1) as single system using MIQP formulation.

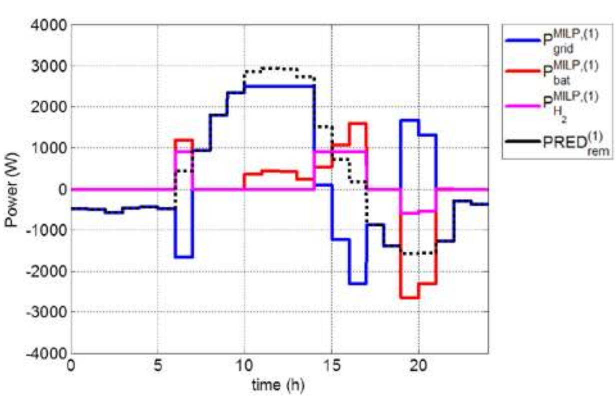

Fig. 5. Day-ahead optimization results obtained for Microgrid (1) as single system using MILP formulation.

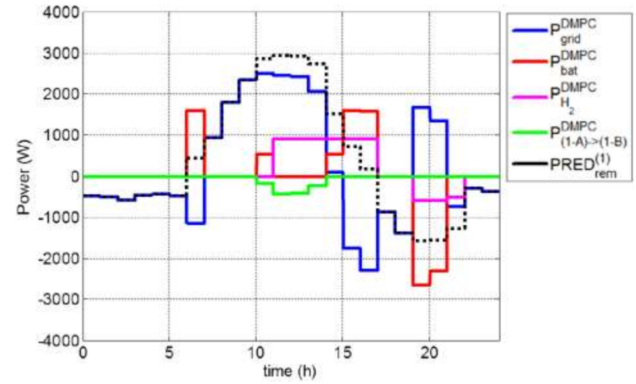

Fig. 6. Day-ahead optimization results obtained for microgrid (1-A) using DMPC.

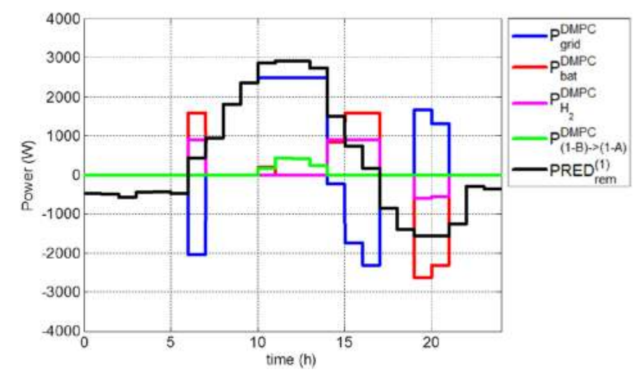

Fig. 7. Day-ahead optimization results obtained for microgrid (1-B) using DMPC.

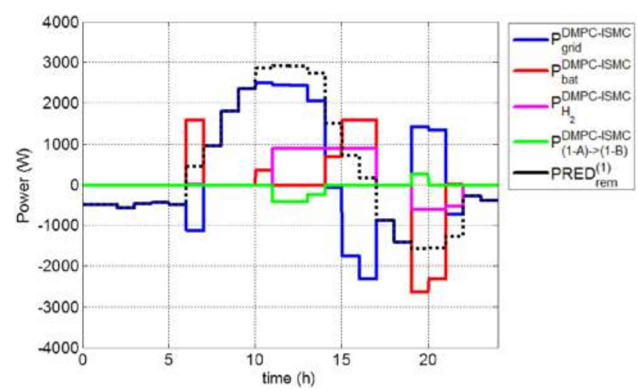

Fig. 8. Day-ahead optimization results obtained for microgrid (1-A) using DMPC including ISMC.

proposed mixed integer linear programming (MILP) formulation is given. As can be seen in Figs. 4 and 5, similar results are obtained. A quantitative comparison for the global cost function and its different parts/terms related to the power exchange with the grid and the cost of use for the batteries and the hydrogen ESS can be found in the first and second column of Table III, where $J_{\text{degr,bat}}^{\text{local}}$ refers to the cost related with the degradation of the batteries, $J_{\text{degr,elz}}^{\text{local}}$ and $J_{\text{degr,fc}}^{\text{local}}$ refers to the costs related to

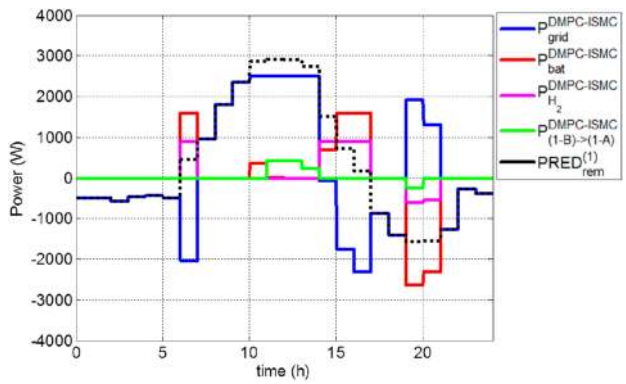

Fig. 9. Day-ahead optimization results obtained for microgrid (1-B) using DMPC including ISMC.

TABLE III
COMPARISON OF THE KEY PERFORMANCE VALUES OF THE CONTROLLERS (DATA EXPRESSED IN € AS UNIT)

	MIQP	MILP	DMPC		DMPC-ISMC	
$J^{local}_{degr,bat}$ (*)	0.0519	0.0526	0.0590	0.0597	0.0592	0.0592
$J^{local}_{degr,elz}$ (*)	0	0	0	0	0	0
$J^{local}_{degr,fc}$ (*)	0	0	0	0	0	0
J^{local}_{grid}	-0.1934	-0.1939	-0.2767	-0.1366	-0.2000	-0.2134
$J^{local}_{cc,bat}$	0.4950	0.4950	0.4950	0.4950	0.4950	0.4950
$J^{local}_{start,fc}$	0.0180	0.0180	0.0180	0.0180	0.0180	0.0180
$J^{local}_{start,elz}$	0.0148	0.0148	0.0074	0.0148	0.0148	0.0074
$J^{local}_{cc,elz}$	0.0296	0.0296	0.0444	0.0296	0.0296	0.0444
$J^{local}_{cc,fc}$	0.0036	0.0036	0.0054	0.0036	0.0036	0.0054
J^{local}_{MIQP} (*)	0.4195	0.4197	0.3524	0.4841	0.4202	0.4160
J^{local}_{MILP}	-	0.4207	-	-	0.4207	0.4165

(*) Evaluated in the MIQP original form [17] with the solution given by each controller

power fluctuations in the fuel cell and the electrolyzer, $J^{\text{local}}_{\text{grid}}$ concerns the economic cost of exchanging power with the grid, $J^{\text{local}}_{\text{degr,bat}}$ refers to the cost related to the number of life cycles used for the batteries, $J^{\text{local}}_{\text{degr,elz}}$ and $J^{\text{local}}_{\text{degr,fc}}$ are the costs due to the number of operation hours of the electrolyzer and the fuel cell, $J^{\text{local}}_{\text{start,elz}}$ and $J^{\text{local}}_{\text{start,fc}}$ compute the costs related to the start up and shut down processes of the electrolyzer and the fuel cell, and $J^{\text{local}}_{\text{MIQP}}$ and $J^{\text{local}}_{\text{MILP}}$ express the sum of all the terms of the cost of the optimization of the whole microgrid.

The results from the formulation of the P2P day-ahead operation of the two microgrids, formulated just as a DMPC problem and formulated integrating the improvement of the single mode criterion (ISMC) are exposed in Figs. 6–9 and in the third–sixth columns of Table III. As can be seen in the row of $J_{\text{total,MIQP}}$, when the problem is formulated as DMPC without the ISMC, microgrid (1-A) improves the economical benefit while microgrid (1-B) has a lower economical benefit, than acting as a single microgrid. When the ISMC is applied, microgrid (1-A) maintains its economical benefit while microgrid (1-B) improves its economical benefit.

B. Day-Ahead Network Controller

The results of the global optimization of the network of microgrids is exposed in Figs. 10–13. The results of the different steps of the algorithm is exposed in Table IV. In the first iteration

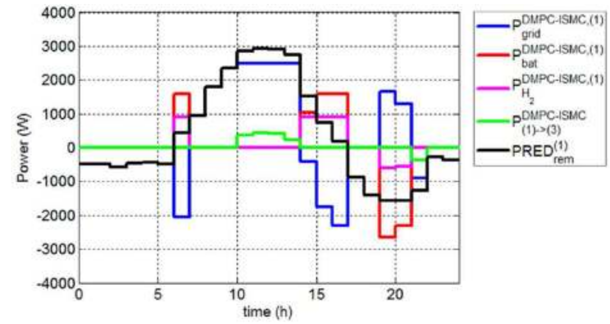

Fig. 10. Day-ahead optimization results obtained for microgrid (1) inside the network using DMPC including ISMC.

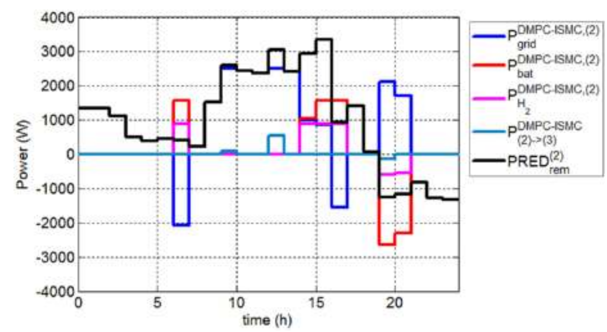

Fig. 11. Optimization results obtained for microgrid (2) inside the network using DMPC including ISMC.

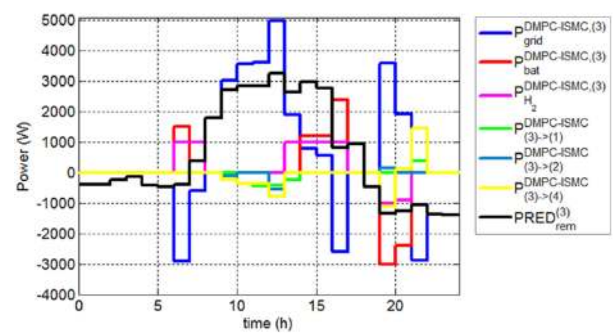

Fig. 12. Day-ahead optimization results obtained for microgrid (3) inside the network using DMPC including ISMC.

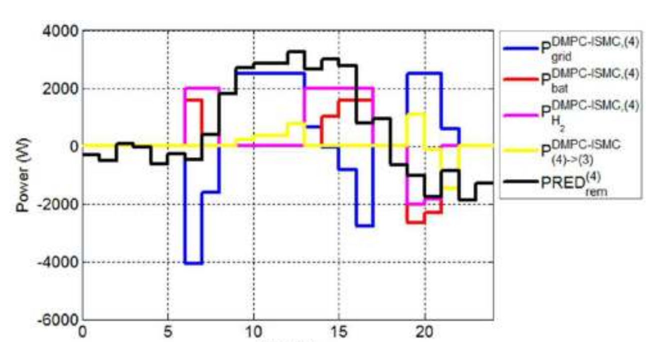

Fig. 13. Day-ahead optimization results obtained for microgrid (4) inside the network using DMPC including ISMC.

TABLE IV
COST FUNCTION VALUES AT THE DIFFERENT ITERATION STEPS OF THE DMPC ALGORITHM APPLIED TO THE NETWORK (DATA EXPRESSED IN € AS UNIT)

ITER: 0	(1)	(2)	(3)	(4)		
J_{single}	0.4207	-1.3100	-0.2122	-0.0904		
ITER: 1	**(1)(2)**	**(1)(3)**	**(1)(4)**	**(2)(3)**	**(2)(4)**	**(3)(4)**
$J_{local,(A)}$	0.4172	0.4207	0.4012	-1.3100	-1.3243	-0.2376
$J_{local,(B)}$	-1.3100	-0.2202	-0.904	-0.2154	-0.0904	-0.0905
ΔJ_{global}	-0.0035	-0.0080	-0.0195	-0.0033	-0.0143	-0.0253
ITER: 2[3,4]	**(1)(2)**	**(1)(3')**	**(1)(4')**	**(2)(3')**	**(2)(4')**	**(3')(4')**
$J_{local,(A)}$	0.4172	0.4207	0.4207	-1.3100	-1.3100	-0.2376
$J_{local,(B)}$	-1.3100	-0.2457	-0.0919	-0.2408	-0.0907	-0.0905
ΔJ_{global}	-0.0035	-0.0082	-0.0014	-0.0033	-0.0002	0
ITER: 3[1,3']	**(1')(2)**	**(1')(3'')**	**(1')(4')**	**(2)(3'')**	**(2)(4')**	**(3'')(4')**
$J_{local,(A)}$	0.4201	0.4207	0.4207	-1.3100	-1.3100	-0.2457
$J_{local,(B)}$	-1.3100	-0.2457	-0.0919	-0.2490	-0.0907	-0.0905
ΔJ_{global}	-0.006	0	0	-0.0033	-0.0002	0
ITER: 4[2,3'']	**(1')(2')**	**(1')(3''')**	**(1')(4')**	**(2')(3''')**	**(2')(4')**	**(3''')(4')**
$J_{local,(A)}$	0.4207	0.4207	0.4207	-1.3100	-1.3100	-0.2490
$J_{local,(B)}$	-1.3100	-0.2490	-0.0919	-0.2490	-0.0905	-0.0905
ΔJ_{global}	0	0	0	0	0	0

of the table (ITER: 0), the cost function of each microgrid acting as single microgrid is shown. In the second iteration (ITER: 1), the different couples of microgrids are evaluated showing the local cost function for each microgrid of the couple acting inside the couple, as well as the increment of benefit of the couple of microgrid. In the third iteration shown in the Table IV (ITER: 2), notice that the path given by the node of the couple [3, 4] is followed by the optimization algorithm as best path. But there exists different branches of the trees given by all the combination possibilities presented in ITER:1. In ITER:3, the followed node is the one given by the couple [1, 3']. Notice that microgrid (3') is the mutation of microgrid (3) after the commitment to energy exchange with microgrid (4) at the previous step. Similar procedure is followed with the mutation of microgrid (4) toward (4'). The terminal node given in the fifth iteration (ITER:4[2, 3'']) does not find any new couple, because $\Delta J_{\text{global}} = 0$ for all the cases. Although, only the optimal path of the tree is shown, but all the branches and nodes should be calculated in order to find the optimal. Notice that not all the microgrids have to exchange energy and it doesn't exist between microgrids (2)–(4) or their mutations along the combinatorial tree in the optimal path given by the algorithm. Only microgrid (3) exchanges energy with all the microgrids of the network having three mutations.

C. Regulation Service P2P

In Fig. 14 and 15, the optimization results of the microgrids (1) and (3) without the exchange of energy in the network in the regulation service schedule step is shown. However, the exchange of energy given by the schedule in the day-ahead step is considered. In Figs. 16 and 17, the optimization results after applying the proposed algorithm are exposed. The evolution of the state variables (SOC_{uc}, SOC_{bat}, and LOH) for each microgrid are exposed in Figs. 18 and 19, finding an equitable increment of gain in the cost function of -2.0377 € for each microgrid. The excess of energy in microgrid (3) is compensated with the deficit of energy in microgrid (1), finding a better tracking of the schedule given in the day-ahead market but in a

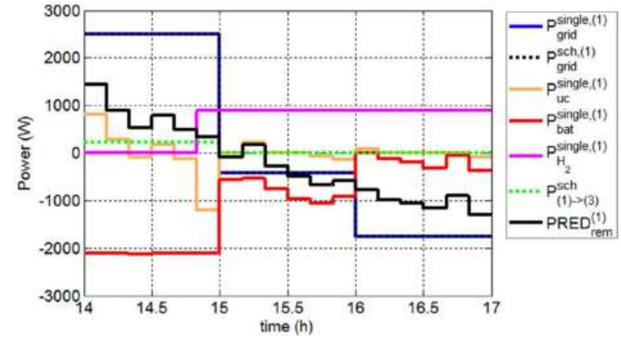

Fig. 14. Regulation-service-market optimization results obtained for microgrid (1) as single microgrid.

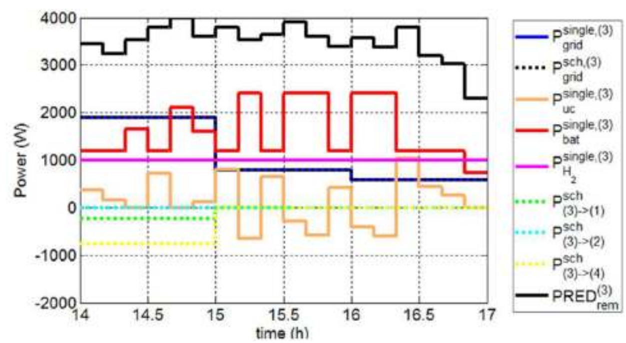

Fig. 15. Regulation-service-market optimization results obtained for microgrid (3) as single microgrid.

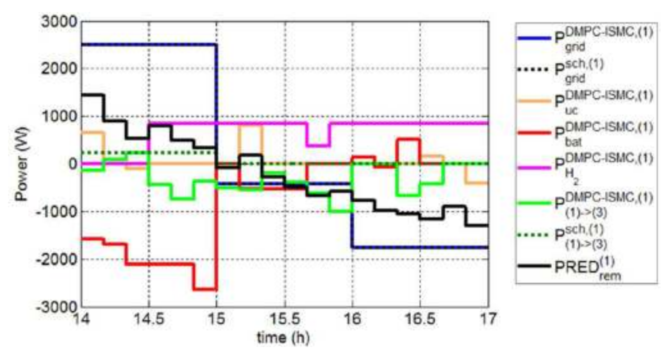

Fig. 16. Regulation-service-market optimization results obtained for microgrid (1) using DMPC optimization.

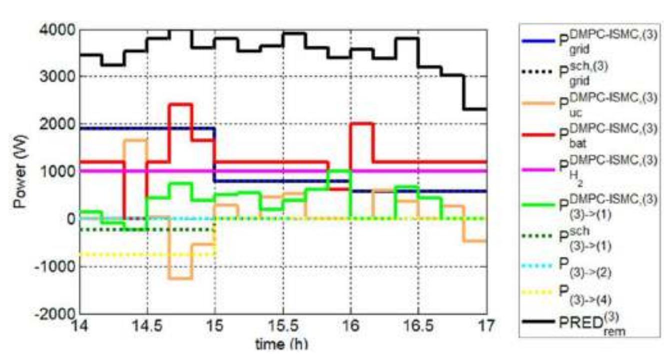

Fig. 17. Regulation-service-market optimization results obtained for microgrid (3) using DMPC optimization.

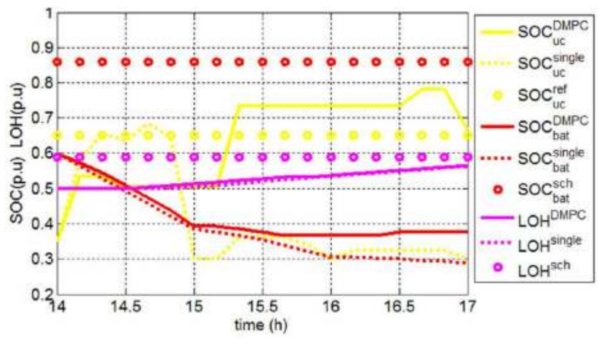

Fig. 18. State variable evolution for microgrid (1) in Regulation Market.

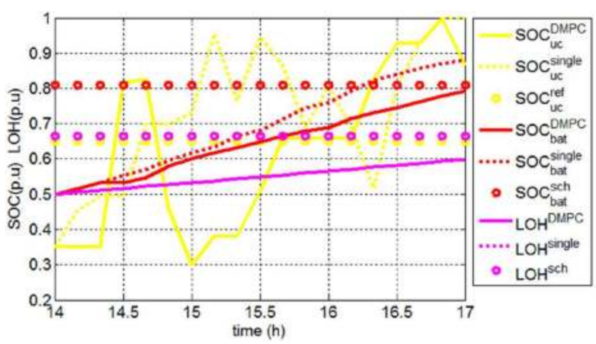

Fig. 19. State variable evolution for microgrid (3) in Regulation Market.

controlled way in order to achieve similar benefits for each microgrid.

V. Conclusion

In this paper, the market operation of four interconnected microgrids was improved through its operation as a network using a DMPC-based algorithm. The methodology carried out guarantees that the optimal operation point of the network implies a similar or better operation point of each microgrid acting as a single system. In order to improve the computational cost of the system, the local controllers of the microgrid formulated as an MIQP problem are linearized and reformulated as an MILP problem. The quadratic terms of the original MIQP problem were linearized under a piecewise approach. Two procedures were presented and validated for the day-ahead market and the regulation service market, introducing the concepts of improvement of the single mode criterion for the case of the day-ahead market and the equitable gain for the regulation service market. Both the concepts can be easily applied to the different schedule levels of the electrical market operation of network of microgrids by just selecting the related constraints. The results presented show that the networked operation of microgrids can improve the economical benefits as compared to the single mode operation. It also helps to maximize the lifetime of the ESS when the cooperation among microgrids can be used to decrease the number of start up/shut down cycles, the number of working hours and power fluctuations of the electrolyzer and fuel cell, or reducing the number of cycles of the batteries and limiting the high values in the charging and discharging process of the batteries.

References

[1] R. Lasseter, "Smart distribution: Coupled microgrids," in *Proc. IEEE*, vol. 99, no. 6, pp. 1074–1082, Jun. 2011.

[2] H. Kumar Nunna and S. Doolla, "Multiagent-based distributed-energy-resource management for intelligent microgrids," *IEEE Trans. Ind. Electron.*, vol. 60, no. 4, pp. 1678–1687, Apr. 2013.

[3] D. Gregoratti and J. Matamoros, "Distributed energy trading: The multiple-microgrid case," *IEEE Trans. Ind. Electron.*, vol. 62, no. 4, pp. 2251–2559, Apr. 2015.

[4] C. Colson and M. H. Nehrir, "Comprehensive real-time microgrid power management and control with distributed agents," *IEEE Trans. Smart Grid*, vol. 4, no. 1, pp. 617–627, Mar. 2013.

[5] M. Fathi and H. Bevrani, "Statistical cooperative power dispatching in interconnected microgrids," *IEEE Trans. Sustain. Energy*, vol. 4, no. 3, pp. 586–593, Jul. 2013.

[6] J. Wu and X. Guan, "Coordinated multi-microgrids optimal control algorithm for smart distribution management system," *IEEE Trans. Smart Grid*, vol. 4, no. 4, pp. 2174–2181, Dec. 2013.

[7] G. Hug, S. Kar, and C. Wu, "Consensus + innovations approach for distributed multiagent coordination in a microgrid," *IEEE Trans. Smart Grid*, vol. 6 , no. 4, pp. 1893–1903, Jul. 2015.

[8] E. Mojica-Nava, C. Barreto, and N. Quijano, "Population games methods for distributed control of microgrids," *IEEE Trans. Smart Grid*, vol. 6, no. 6, pp. 2586–2595, Nov. 2015.

[9] J. M. Maestre and R. R. Negenborn, *Distributed Model Predictive Control Made Easy.* New York, NY, USA: Springer, 2014.

[10] R. R. Negenborn, "Multi-agent model predictive control with applications to power networks," Ph.D. dissertation, Delft Univ., Delft, The Netherlands, 2007.

[11] A. Parisio, C. Wiezorek, T. Kyntäjä, J. Elo, K. Strunz, and K. H. Johansson, "Cooperative MPC-based energy management for networked microgrids," *IEEE Trans. Smart Grid*, vol. 8, no. 6, pp. 3066–3074, Nov. 2017.

[12] F. J. Muros, J. M. Maestre, E. Algaba, T. Alamo, and E. F. Camacho, "An iterative design method for coalitional control networks with constraints on the shapley value," in *Proc. 19th IFAC World Congr.*, Cape Town, South Africa, 2014, pp. 1188–1193.

[13] A. J. Del Real, A. Arce, and C. Bordons, "An integrated framework for distributed model predictive control of large-scale power networks," *IEEE Trans. Ind. Inform.*, vol. 10, no. 1, pp. 197–209, Feb. 2014.

[14] A. Ouammi, H. Dagdougui, L. Dessaint, and R. Sacile, "Coordinated model predictive-based power flows control in a cooperative network of smart microgrids," *IEEE Trans. Smart Grid*, vol. 6, no. 5, pp. 2233–2244, Sep. 2015.

[15] W. Qi, J. Liu, and P. D. Christofides, "Distributed supervisory predictive control of distributed wind and solar energy generation systems," *IEEE Trans. Control Syst. Technol.*, vol. 21, no. 2, pp. 504–512, Mar. 2013.

[16] M. R. Sandgani and S. Sirouspour, "Coordinated optimal dispatch of energy storage in a network of grid-connected microgrids," *IEEE Trans. Sustain. Energ.*, vol. 8, no. 3, pp. 1166–1176, Jul. 2017.

[17] F. Garcia-Torres and C. Bordons, "Optimal economical schedule of hydrogen-based microgrids with hybrid storage using model predictive control," *IEEE Trans. Ind. Electron.*, vol. 62, no. 8, pp. 5195–5207, Aug. 2015.

[18] F. Garcia-Torres and C. Bordons, "Optimal load sharing of hydrogen-based microgrids with hybrid storage using model predictive control," *IEEE Trans. Ind. Electron.*, vol. 63, no. 8, pp. 4919–4928, Aug. 2016.

[19] R. Steinmetz and K. Wehrle, "What is this peer-to-peer about?," in *Peer-to-Peer Systems And Applications*. New York, NY, USA: Springer-Verlag, 2005.

[20] *DOE. Hydrogen and Fuel Cells Program Record 14012* , U.S. Department of Energy (DOE), Washington, DC, USA.

[21] *DOE. Multi-Year Research, Development and Demonstration Plan (Hydrogen Production)*, U.S. Department of Energy (DOE)Washington, DC, USA.

[22] D. Howell, "Battery status and cost reduction prospects," in *Proc. EV Everywhere Grand Challenge Battery Workshop*, July 2012. [Online]. Available: https://www1.eere.energy.gov/vehiclesandfuels/pdfs/ev_everywhere/5_howell_b.pdf

Felix Garcia-Torres was born in Cordoba, Spain, in 1977. He received the Ph.D. degree in electrical engineering from the University of Seville, Seville, Spain, in 2015.

In 2009, he joined the Centro Nacional del Hidrogeno, Puertollano, Spain, where he is currently working as an incharge of the Microgrids Laboratory in the Simulation and Control Unit. Previously, he was working in several research centers or companies such as the Instituto de Automatica Industrial-Consejo Superior de Investigaciones Cientificas, Madrid, Spain, the University of Seville spin-off GreenPower Technologies, Seville, Spain, and the Université Catholique de l'Ouest, Angers, France. His research interests include advanced power electronics and control to introduce energy storage technologies in the smart grid.

Carlos Bordons (M'98–SM'17) was born in Seville, Spain, in 1962. He received the Ph.D. degree in industrial engineering from the University of Seville, Seville, in 1994.

He joined the Escuela Superior de Ingenieria of Seville, Seville, as an Assistant Professor in 1996 and he is currently working there as a Full Professor of Systems Engineering and Automatic Control. From 2013 to 2017, he was the Head of the Systems Engineering and Automatic Control Department with the University of Seville. His research interests include advanced process control, especially model predictive control and its application to energy systems. His recent work is focused on power management in hybrid vehicles and control of microgrids including renewable sources.

Miguel A. Ridao (M'98) received the Ph.D. degree in industrial engineering from the University of Seville, Seville, Spain, in 1996.

He is an Associate Professor of System Engineering and Automation with the Engineering School of the University of Seville. He has worked in different projects in collaboration with the industry in fields such as control of power management in hybrid vehicles, control of microgrids including renewable sources, simulation and optimization of oil pipeline networks, and risk management. His research interests include distributed control, control of water systems, simulation, hybrid vehicles including fuel cells, automation of supply channels, and decision support systems.